Brief Communications

PHR Regulates Growth Cone Pausing at Intermediate Targets through Microtubule Disassembly

Michael Hendricks[1] **and Suresh Jesuthasan**[1,2]

[1]Temasek Life Sciences Laboratory, The National University of Singapore, Singapore 117604, and [2]Biomedical Sciences Institutes, Neuroscience Research Partnership, Singapore 138673

Axonal growth cones use intermediate targets to navigate in the developing nervous system. Encountering these sites is correlated with growth cone pausing. PHR (Phr1, Esrom, Highwire, RPM-1) is a large neuronal ubiquitin ligase that interacts with multiple signaling pathways. Mouse and zebrafish *phr* mutants have highly penetrant axon pathfinding defects at intermediate targets. Mouse *phr* mutants contain excessive microtubules in the growth cone, which has been attributed to upregulation of DLK/p38 signaling. Here, we ask whether this pathway and microtubule misregulation are indeed linked to guidance errors in the vertebrate brain, using the zebrafish. By live imaging, we show that loops form when microtubules retract without depolymerizing. JNK, but not p38, phosphorylation is increased in mutant growth cones. However microtubule looping cannot be suppressed by inhibiting JNK. The *phr* microtubule defect can be phenocopied by taxol, while microtubule destabilization *in vitro* using nocodazole prevents loop formation. Acute disruption *in vivo* with nocodazole suppresses the intermediate target guidance defect. Given that microtubule looping is associated with growth cone pausing, we propose that microtubule disassembly, mediated by PHR, is essential for exiting the paused state at intermediate targets.

Introduction

Growing axons follow long paths that are broken up into smaller segments by intermediate targets. Typically, growth cones slow down or pause at these sites, while undergoing changes in morphology and signaling properties. Recent studies have described defects in axon pathfinding at intermediate targets, caused by mutations affecting microtubules and their associated proteins (Rothenberg et al., 2003; Lee et al., 2004, 2007), indicating that many guidance cues acting at intermediate targets regulate the microtubule cytoskeleton.

The PHR family of proteins includes human PAM, mouse Phr1, zebrafish Esrom, *Drosophila* Highwire, and *Caenorhabditis elegans* RPM-1 (Guo et al., 1998; Schaefer et al., 2000; Wan et al., 2000; Zhen et al., 2000; Burgess et al., 2004; D'Souza et al., 2005); for clarity we will refer to these as PHR. In vertebrates, *phr* mutants show highly specific axon pathfinding errors, which can be described as a failure to negotiate certain intermediate targets (Bloom et al., 2007; Lewcock et al., 2007; Hendricks et al., 2008). PHR is a huge, multidomain protein, and in invertebrates has been shown to regulate synapse formation via dual leucine zipper-bearing kinase (DLK), a member of the mixed lineage kinase (MLK) family of MAP3Ks, through its ubiquitin ligase activity (Nakata et al., 2005; Collins et al., 2006). In *C. elegans*, PHR is required for DLK-mediated activation of p38 MAP kinase (Nakata et al., 2005), whereas in *Drosophila* DLK acts via c-Jun N-terminal kinase (JNK) (Collins et al., 2006).

Cultured spinal neurons from *phr* mutant mice display growth cones with abnormal morphologies and disorganized microtubules (Lewcock et al., 2007). Since DLK was found away from the axon tip in *phr* mutants, and inhibition of p38 or treatment with taxol reduced microtubule disorganization, it was proposed that PHR acts outside of growth cones to stabilize microtubules by mediating destruction of DLK. However, loss of DLK fails to suppress axon pathfinding defects in the *phr* mutant mouse, and no increase in DLK was detected in *phr* mutants (Bloom et al., 2007). Furthermore, misregulation of p38 has not been demonstrated in PHR mutants. It is thus unclear whether and how the microtubule phenotype is linked to the pathfinding defect, or indeed, if microtubule regulation by PHR is mediated by DLK/p38 signaling.

The zebrafish *phr* mutant has a striking pathfinding defect in the dorsal forebrain (Hendricks et al., 2008). Axons that are destined to form the habenular commissure navigate normally to an intermediate target adjacent to the roof plate, but stall indefinitely and fail to cross the midline. Here, we use the zebrafish to test whether disorganized microtubules underlie the guidance defect at intermediate targets in *phr* mutants, and whether this occurs via overactivation of p38 or JNK.

Materials and Methods

Forebrain cultures. Primary forebrain culture was performed as described previously (Hendricks and Jesuthasan, 2007). Microtubule immunofluorescence was based on Mitchison Lab protocols (http://mitchison.med.harvard.edu/protocols/gen1.html). Cultures were fixed for 10 min in microtubule fix [0.5% glutaraldehyde, 0.1% Triton X-100, and BRB80 (80 mM PIPES, pH 6.8, 1 mM $MgCl_2$, and 1 mM EGTA)] and quenched

Received March 7, 2009; accepted April 6, 2009.

This work was funded by the Singapore Millennium Foundation and the Biomedical Research Council. We thank Erik Dent and Ajay Mathuru for comments on the manuscript.

Correspondence should be addressed to Suresh Jesuthasan, Biomedical Sciences Institutes, Neuroscience Research Partnership, 04-13B Proteos, 61 Biopolis Drive, Singapore 138673. E-mail: suresh.jesuthasan@nrp.a-star.edu.sg.

M. Hendricks' present address: Department of Organismic and Evolutionary Biology, Center for Brain Science, Room 254, 52 Oxford Street, Northwest Science Building, Harvard University, Cambridge, MA 02138.

DOI:10.1523/JNEUROSCI.1115-09.2009

 0270-6474/09/296593-06$15.00/0

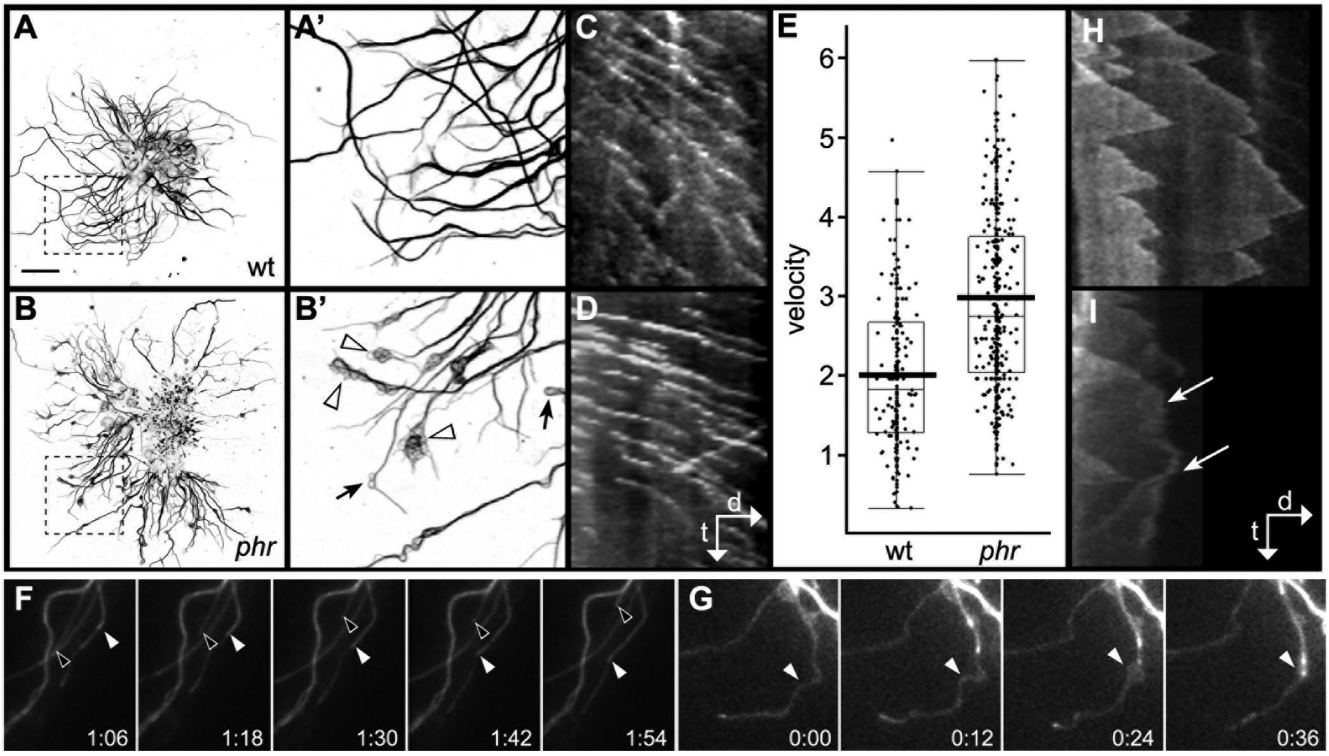

Figure 1. Microtubules in *phr* mutant axons. ***A***, ***B***, Forebrain explants from wild-type and *phr* embryos, α-tubulin immunofluorescence. Areas of insets (***A′***, ***B′***) are shown with dashed lines. Microtubules in mutants exhibit small single or double loops (arrows) as well as large tangles (arrowheads). Kymograph analysis shows more rapid translocation of EB3-EGFP-positive microtubule plus-ends in mutants (***D***) compared with wild type (***C***) (Mann–Whitney *U* test, $p < 0.01$), as indicated by the slope of the puncta. ***E***, Plot of all measured puncta showing quartile divisions of plus-end growth rate (slope), heavy bars show mean values. ***F***, Frames from a time-lapse recording of wild-type axons with a moderate level of EB3 label. Microtubules grow and shrink (arrowheads indicate tips), without coil formation. This behavior is reflected in the kymograph (***H***) made from another wild-type axon. ***G***, Mutant axons. The microtubule coils proximally (arrowhead) while the tip remains relatively stationary. ***I***, Kymograph of a different mutant axon, again showing reduced shrinkage. A coil formed at the point indicated by the upper arrow. The microtubule retracted at the point indicated by the lower arrow. See supplemental material (available at www.jneurosci.org). In kymographs, d indicates distance and t indicates time. Scale bar, 20 μm.

with 0.1% sodium borohydrate for 7 min. For phospho-p38, fixation was done in 4% PFA, 20% sucrose, and PBS for 20 min at 4°C. For phospho-JNK and phospho-cJUN label, a 10 min fixation was performed in microtubule fix supplemented with 3.7% formaldehyde. Details on antibodies used are provided in the supplemental material (available at www.jneurosci.org).

Electroporation. pNBT:EB3-EGFP, which contains the neuronal β-tubulin promoter driving EGFP-EB3 fusion (gift from Vincent Cunliffe, University of Sheffield, Sheffield, UK), was injected into the forebrain. Electrodes (PBSA0575, FHC) were used to apply several 30 V, 1 ms pulses from a Grass (Warwick) Telefactor SD9 voltage stimulator (Hendricks and Jesuthasan, 2007).

Pharmacology. Stock solutions of SP600125 (Tocris) and SB203580 (Merck), were prepared at a concentration of 100 and 50 mM respectively, in cell culture grade DMSO (Sigma). Both compounds have previously been used on zebrafish (Fujii et al., 2000; Zhu et al., 2008).

Brains were injected with glass capillary needles made using a Sutter needle puller (Novato). Embryos at 2 dpf were mounted in agarose and a Narishige air pressure injector was used to deliver several picoliters of 0.33 μM nocodazole (in Ringers/10% DMSO) into the forebrain. The following day, embryos were fixed in 2% trichloroacetic acid/1% Triton X-100/PBS, washed, and stained with a monoclonal anti-acetylated tubulin antibody (1:1000, Sigma).

Imaging. Cultures were imaged live on a Zeiss Axiovert microscope with a 100× phase objective (NA 1.4, Zeiss). Time-lapse images were acquired every 3 s with a Photometrics Cascade CCD camera using MetaMorph software. Fixed cultures were imaged on an inverted Zeiss LSM510 Meta confocal with a 63× oil-immersion lens. Whole mounts were imaged on either an upright Zeiss LSM510 or Exciter confocal using a 40× water-dipping objective.

Details on image analysis are provided in the supplemental material (available at www.jneurosci.org).

Results

Microtubules in *phr* mutant axons have an overgrowth phenotype

When forebrain neurons from zebrafish *phr* mutants were placed in culture, heterogeneous microtubule defects were observed in many axons (Fig. 1*A*,*B*). These included single or clustered loops along the axon shaft, as well as complex snarls within growth cones.

To examine the mechanistic underpinnings of these defects, we performed time-lapse recordings of axons expressing the plus-end binding protein EB3 fused to EGFP. Typical "comets" corresponding to growing microtubules were observed in wild-type and mutant axons. Kymographic analysis of time-lapse videos revealed that plus-end translocation was significantly more rapid in mutants (Fig. 1*C–E*). Average time for growth, as measured by persistence of EB3 signal, was the same in mutant and wild type: 8.8 ± 0.5 and 8.4 ± 0.6 respectively (number of frames ± SE, $n = 42$). This implies that longer polymers were assembled in mutants.

Neurons with a moderate level of EB3-EGFP, such that the entire microtubule was dimly labeled while the growing tip was more strongly fluorescent, allowed us to observe microtubule loops forming. In wild-type neurons ($n = 5$), microtubules grew slowly and shrank rapidly (Fig. 1*F*,*H*; supplemental Movie 1, available at www.jneurosci.org as supplemental material), characteristic features of dynamic instability (Mitchison and Kirschner, 1984). In mutants ($n = 6$) with a similar or lower level of expression, growth was sometimes followed by little or no retraction, and this was accompanied by buckling and looping of the

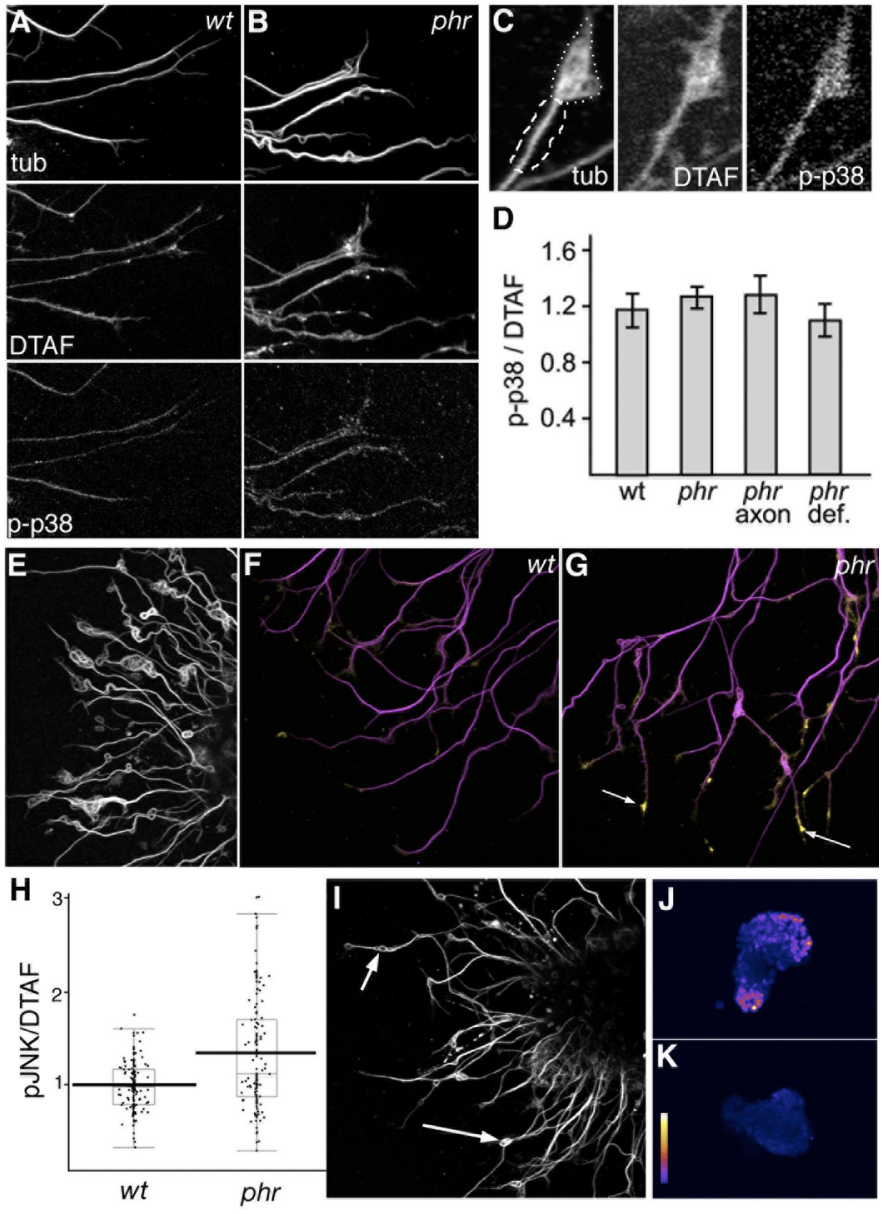

Figure 2. Phosphorylation of p38 and JNK in *phr* mutants. ***A***, ***B***, Cultured wild-type and mutant forebrain axons labeled with anti-α-tubulin, DTAF (total protein), and anti-phospho-p38. ***C***, Higher magnification of a mutant axon, showing an example of regions of analysis used for measuring the phospho-p38:DTAF ratio in normal (dashed line) versus defective (dotted line) microtubule areas. ***D***, The proportion of phospho-p38:DTAF does not very between mutant and wild-type axons, and is the same in looped/disorganized regions as in adjacent areas of the axon. Bars indicate SEM. ***E***, Mutant neurons after treatment with 50 μM SB203580. Microtubules, labeled with anti-α-tubulin, form loops in the axon. ***F***, ***G***, Wild-type and mutant forebrain neurons labeled with anti-α-tubulin (magenta) and anti-phospho-JNK (yellow). Arrows indicate growth axon tips with visible increase in phospho-JNK immunofluorescence. ***H***, Ratio of phospho-JNK to DTAF in wild-type and mutant growth cones The plot shows quartile divisions of values and heavy bars indicate mean values. ***I***, *phr* mutant axons, labeled for α-tubulin, following treatment with 20 μM SP600125. Loops are indicated by arrowheads. ***J***, ***K***, Assessment of SP600125 efficacy by analysis of phosphorylation of cJUN, a target of JNK. Levels of phospho-cJUN are high in control explants (0.1% DMSO; ***J***), and lower in explants treated with 20 μM SP600125 (***K***). Images are pseudocolored, with white representing the highest intensity, as indicated by the wedge.

microtubule filament proximal to the plus-end (Fig. 1*G*,*I*; supplemental Movie 2, available at www.jneurosci.org as supplemental material). Microtubules that formed subsequently polymerized along these loops.

JNK signaling is overactivated in *phr* mutant growth cones

Increased signaling via p38 has been proposed to cause the microtubules defects in mouse *phr* mutants. To test whether this pathway is overactivated in zebrafish mutants, we labeled cultured forebrain neurons with an antibody against active p38. No increase in label was observed in growth cones of mutants, compared with wild-type siblings (Fig. 2*A*,*B*,*D*). There was no correlation between the level of phospho-p38 and the presence of microtubule defects (Fig. 2*C*,*D*). Treatment of cultured axons with the p38 inhibitor SB203580 did not prevent the formation of microtubule loops (Fig. 2*E*).

We next examined JNK, another MAP kinase that may be regulated by PHR. In contrast to p38, levels of phospho-JNK were elevated in mutant growth cones (Fig. 2*F–H*). However, treatment of cultures with 2, 4, 10, or 20 μM SP600125 did not prevent loop formation (Fig. 2*I*). These concentrations caused a reduction in phosphorylated c-JUN (Fig. 2*J*,*K*), confirming that the drug was inhibiting JNK. Hence, upregulation of JNK in the *phr* mutant does not appear to be a critical factor in the formation of microtubule loops.

phr defects are phenocopied by taxol and suppressed by nocodazole

Live imaging of microtubules suggested that increased polymerization and/or stability might contribute to the microtubule defects in *phr* mutants. Consistent with this, treatment of wild-type forebrain explants with taxol, a compound that can increase the rate of tubulin polymerization in cells (De Brabander et al., 1981) and stabilize microtubules, resulted in the formation of numerous loops and knotted microtubule structures within axons and growth cones (Fig. 3*C*,*D*,*G*). Microtubules were then examined for detyrosination (Fig. 3*H–K*), a posttranslational modification that occurs gradually and is thus normally found in stable microtubules, e.g., primarily in the axon shaft. Twenty-one of 189 mutant axon tips contained this marker, in contrast to only two of 120 wild-type axons tips, indicating that a small proportion of mutant growth cones contain stabilized microtubules.

When treated with 20 nM nocodazole, which inhibits assembly of tubulin polymers and promotes microtubule depolymerization (Samson et al., 1979), *phr* cultures showed significant reduction in the proportion of axons displaying microtubule abnormalities (Fig. 3*E–G*); this treatment had no effect on wild-type axons. Higher concentrations (50 nM) prevented axon outgrowth, while lower concentrations (10 nM) had no effect (data not shown).

Nocodazole suppresses habenular commissure defects

To test whether abnormal microtubule stability underlies the defect in habenular commissure formation, we treated mutants

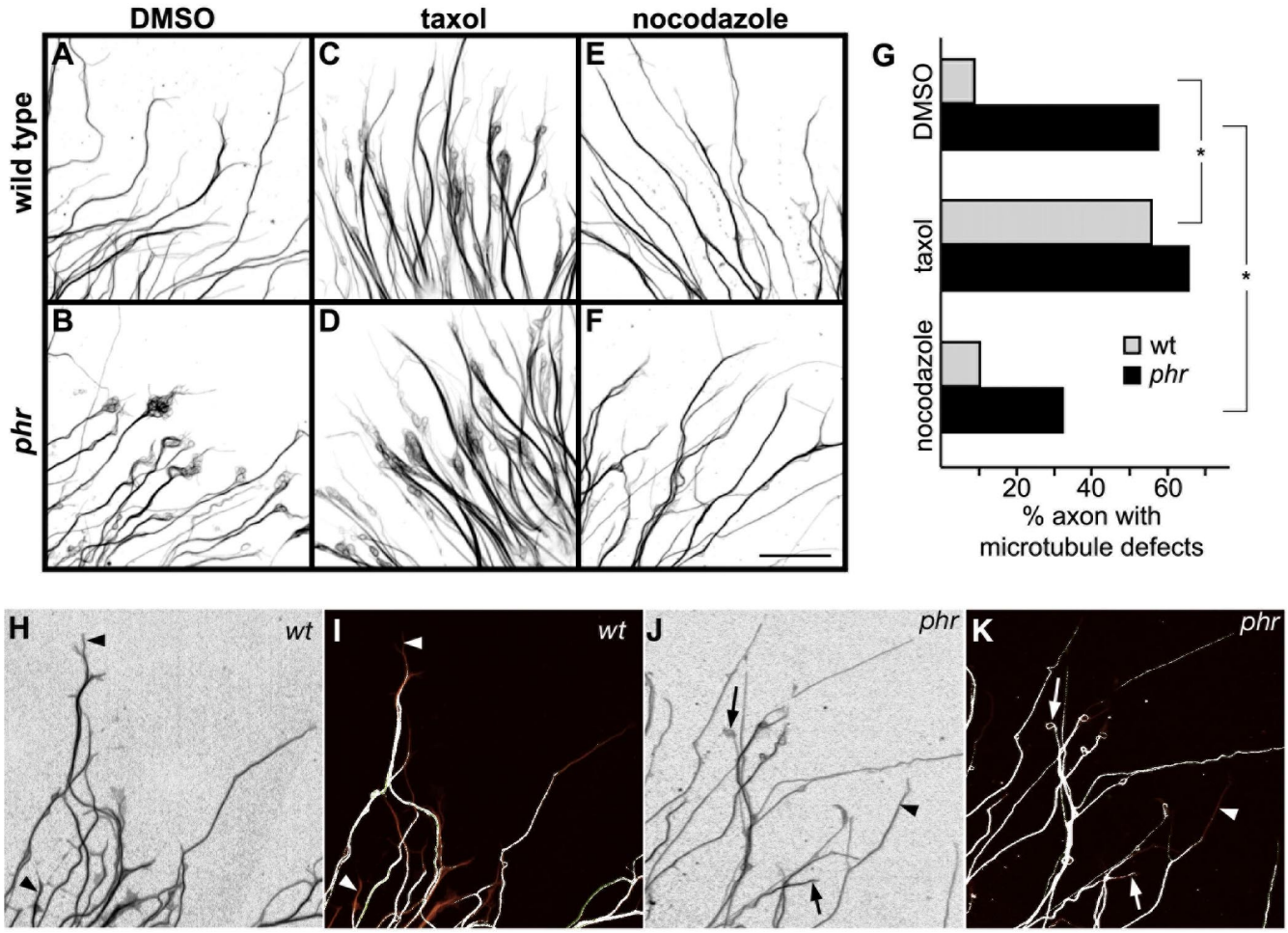

Figure 3. Phenocopy and suppression of microtubule defects. ***A***, ***B***, Control cultures treated with DMSO ($n_{wt} = 276$, $n_{phr} = 150$). ***C***, ***D***, Overnight treatment with 20 nM taxol phenocopies the microtubule looping seen in *phr* ($n_{wt} = 156$, $n_{phr} = 106$). ***E***, ***F***, Nocodazole treatment leads to a reduction in microtubule defects ($n_{wt} = 71$, $n_{phr} = 78$). ***G***, Proportion of axons showing one or more microtubule defects (single or multiple loops) (*χ^2 test, $p < 0.001$). ***H–K***, Double label for total (***H***, ***J***) and detyrosinated tubulin. Regions containing detyrosinated tubulin are indicated in white in panels I and K. Arrowheads indicate axon tips containing low levels of detyrosinated tubulin, whereas arrows indicate axon tips with high levels of detyrosinated tubulin.

with acute doses of nocodazole at 48–52 hpf, when many axons have reached the intermediate target and stalled. Nocodazole was injected directly into the forebrain, and the following day embryos were assayed for commissure formation (Fig. 4). Control mutant siblings showed midline crossing in ~10% of cases, consistent with the previously reported penetrance of the allele used here, phr^{tg06} (Hendricks et al., 2008). Approximately one-third of mutants injected with nocodazole (15/43) showed phenotypic suppression. Results were significantly different in two independent experiments ($n = 15$ and $n = 28$, χ^2 test, $p < 0.001$). This suggests that PHR's role in regulating the microtubule cytoskeleton is essential for guidance at the midline.

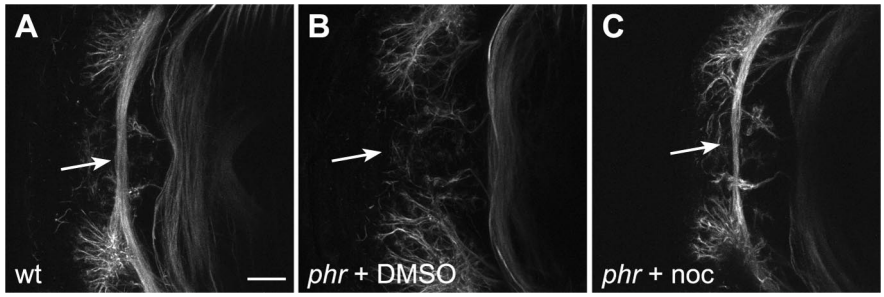

Figure 4. Nocodazole rescues the habenular commissure defect in *phr* mutants. ***A***, Habenular commissure (arrow) of a 3 dpf wild-type embryo labeled for acetylated tubulin. ***B***, The commissure is absent in *phr* mutants. ***C***, Rescue of habenular commissure formation in an embryo injected with nocodazole at 2 dpf. Scale bar, 20 μm.

Discussion

Microtubules and intermediate targets

Growth cones often pause at intermediate targets, becoming larger and less polarized. Enlarged, paused growth cones *in vitro* as well as those at intermediate targets *in vivo* are characterized by an increase in microtubules and microtubule loops (Tsui et al., 1984; Sabry et al., 1991; Tanaka and Kirschner, 1991; Suh et al., 2004). This increase can occur when plus-ends are overstabilized, for example by overexpression of the tip-binding protein CLASP, or when the destabilizing protein SCG10 is inhibited, and this slows growth cone advance (Lee et al., 2004; Suh et al., 2004). Microtubule looping thus appears to be a cause, rather than an effect, of growth cone pausing.

Within growth cones, microtubules are variably coupled to retrograde actin flow (Forscher and Smith, 1988; Schaefer et al.,

2002). The force produced by actin movements can cause microtubules to fold, buckle, or break, and this compression is a mechanism for loop formation (Tanaka and Kirschner, 1991). Recent work suggests the extent of microtubule retrotranslocation by actin can regulate growth cone advance. As coupling or local retrograde flow is decreased, microtubules can extend peripherally and stabilize nascent growth cone processes (Lee and Suter, 2008; Schaefer et al., 2008). If this model is correct, then tight coupling of microtubules to retrograde actin flow may be a mechanism to induce looping, and therefore pausing, at sites such as intermediate targets.

phr mutants and the tubulin cytoskeleton

In zebrafish *phr* mutants, forebrain axons exhibit extensive microtubule looping, similar to those observed in mouse spinal neurons *in vitro* (Lewcock et al., 2007). The formation of loops and growth cones with knotty microtubule arrays has been described in neurons treated with taxol (Letourneau and Ressler, 1984; Williamson et al., 1996; Rajnicek et al., 2006). Chronic treatment with a low dose of taxol indeed phenocopies these aspects of the *phr* phenotype in our forebrain cultures. To the contrary, Lewcock et al. (2007) observed a reduction in growth cone microtubules and their disorganization using a similar taxol treatment. This difference may have occurred because the effects of taxol vary according to concentration, and the effective dose differs according to culture medium, culturing temperature, species, and cell type (see for example Yvon et al., 1999).

Despite the prevalence of microtubule defects in cultured *phr* neurons, the *in vivo* axon guidance phenotypes are highly specific and most axonal projections are normal. For this reason, it is unlikely that *phr* growth cones have general defects in chemotaxis or motility. We suggest that when growth cones encounter sites where microtubule regulation is critical, pathfinding fails. At the roof plate boundary in the zebrafish diencephalon, a Wnt-expressing intermediate target for commissural axons, growth cones normally pause and enlarge before crossing. Wnt can regulate axonal microtubules and induce growth cone enlargement via multiple pathways (Gordon-Weeks, 2004; Ciani and Salinas, 2007; Purro et al., 2008; Salinas and Zou, 2008). We suggest that the additive effects of Wnt signaling at the intermediate target and increased microtubule polymerization and stability in *phr* mutants cause excessive microtubule looping, preventing growth cones from exiting the paused state.

How does PHR regulate microtubules?

In *Drosophila* and *C. elegans,* PHR inhibits a conserved MAP kinase cascade consisting of DLK, MKK4, and p38 or JNK (Nakata et al., 2005; Collins et al., 2006). In the zebrafish, levels of phospho-JNK are visibly increased in mutants. However, JNK does not appear to be involved in the formation of loops, as inhibition with SP600125 does not prevent loop formation. This is in agreement with Bloom et al. (2007), who find that loss of DLK, which can activate JNK, cannot suppress the guidance phenotype in mouse *phr* mutants. Lewcock et al. (2007) have suggested that PHR regulates microtubules via p38, downstream of DLK. We find no evidence of increased p38 signaling in the zebrafish *phr* mutant. This may reflect species or tissue differences; alternatively, the reduction in microtubules caused by p38 inhibition in mouse *phr* growth cones may have been caused by inhibition of a parallel pathway. Consistent with this, treatment of wild-type mouse growth cones with SB203580 caused a reduction in microtubules (Lewcock et al., 2007), and treatment of the mutant only resulted in a partial reduction.

PHR may function within a complex that directly interacts with the cytoskeleton. Intriguingly, the N terminus of PHR shows high homology to the yeast ATS1 (α-tubulin suppressor 1) protein, which reduces microtubule levels through an unknown mechanism (Kirkpatrick and Solomon, 1994). Lewcock et al. (2007) demonstrated that PHR remains associated with the microtubule cytoskeleton after detergent extraction, and recent work by Pierre et al. (2008) shows association with actin. While the former study suggested that PHR is excluded from the growth cone and functions in the axon, the latter shows growth cone localization in mouse spinal neurons. We also observed PHR in the growth cones of both retinal ganglion cells and forebrain neurons in zebrafish, by immunofluorescence (D'Souza et al., 2005; Hendricks et al., 2008).

We hypothesize that PHR acts in the growth cone to regulate microtubule polymerization and stability. This is in contrast to the model of Lewcock et al. (2007), which proposes that PHR is excluded from the growth cone, and in its absence DLK is activated away from the axon tip. We suggest that in the absence of PHR, microtubule dynamics are biased toward growth and may be excessively coupled to actin flow, causing inappropriate looping and a failure to exit a paused state. As predicted by this model, these microtubule defects are phenocopied by taxol and suppressed by nocodazole. Most strikingly, nocodazole rescues growth cone stalling at an intermediate target, constituting the first *in vivo* suppression of *phr* axon guidance defects. In summary, our results demonstrate that microtubule disorganization causes the *phr* guidance phenotype, provide further evidence that microtubule polymerization is causal to growth cone pausing, and suggest that PHR-mediated regulation of microtubule stability is critical to pathfinding at intermediate targets.

References

Bloom AJ, Miller BR, Sanes JR, DiAntonio A (2007) The requirement for Phr1 in CNS axon tract formation reveals the corticostriatal boundary as a choice point for cortical axons. Genes Dev 21:2593–2606.

Burgess RW, Peterson KA, Johnson MJ, Roix JJ, Welsh IC, O'Brien TP (2004) Evidence for a conserved function in synapse formation reveals Phr1 as a candidate gene for respiratory failure in newborn mice. Mol Cell Biol 24:1096–1105.

Ciani L, Salinas PC (2007) c-Jun N-terminal kinase (JNK) cooperates with Gsk3beta to regulate Dishevelled-mediated microtubule stability. BMC Cell Biol 8:27.

Collins CA, Wairkar YP, Johnson SL, DiAntonio A (2006) Highwire restrains synaptic growth by attenuating a MAP kinase signal. Neuron 51:57–69.

De Brabander M, Geuens G, Nuydens R, Willebrords R, De Mey J (1981) Taxol induces the assembly of free microtubules in living cells and blocks the organizing capacity of the centrosomes and kinetochores. Proc Natl Acad Sci U S A 78:5608–5612.

D'Souza J, Hendricks M, Le Guyader S, Subburaju S, Grunewald B, Scholich K, Jesuthasan S (2005) Formation of the retinotectal projection requires Esrom, an ortholog of PAM (protein associated with Myc). Development 132:247–256.

Forscher P, Smith SJ (1988) Actions of cytochalasins on the organization of actin filaments and microtubules in a neuronal growth cone. J Cell Biol 107:1505–1516.

Fujii R, Yamashita S, Hibi M, Hirano T (2000) Asymmetric p38 activation in zebrafish: its possible role in symmetric and synchronous cleavage. J Cell Biol 150:1335–1348.

Gordon-Weeks PR (2004) Microtubules and growth cone function. J Neurobiol 58:70–83.

Guo Q, Xie J, Dang CV, Liu ET, Bishop JM (1998) Identification of a large Myc-binding protein that contains RCC1-like repeats. Proc Natl Acad Sci U S A 95:9172–9177.

Hendricks M, Jesuthasan S (2007) Electroporation-based methods for in vivo, whole mount and primary culture analysis of zebrafish brain development. Neural Dev 2:6.

Hendricks M, Mathuru AS, Wang H, Silander O, Kee MZ, Jesuthasan S (2008) Disruption of Esrom and Ryk identifies the roof plate boundary as an intermediate target for commissure formation. Mol Cell Neurosci 37:271–283.

Kirkpatrick D, Solomon F (1994) Overexpression of yeast homologs of the mammalian checkpoint gene RCC1 suppresses the class of alpha-tubulin mutations that arrest with excess microtubules. Genetics 137:381–392.

Lee AC, Suter DM (2008) Quantitative analysis of microtubule dynamics during adhesion-mediated growth cone guidance. Dev Neurobiol 68:1363–1377.

Lee H, Engel U, Rusch J, Scherrer S, Sheard K, Van Vactor D (2004) The microtubule plus end tracking protein Orbit/MAST/CLASP acts downstream of the tyrosine kinase Abl in mediating axon guidance. Neuron 42:913–926.

Lee S, Nahm M, Lee M, Kwon M, Kim E, Zadeh AD, Cao H, Kim HJ, Lee ZH, Oh SB, Yim J, Kolodziej PA, Lee S (2007) The F-actin-microtubule crosslinker Shot is a platform for Krasavietz-mediated translational regulation of midline axon repulsion. Development 134:1767–1777.

Letourneau PC, Ressler AH (1984) Inhibition of neurite initiation and growth by taxol. J Cell Biol 98:1355–1362.

Lewcock JW, Genoud N, Lettieri K, Pfaff SL (2007) The ubiquitin ligase Phr1 regulates axon outgrowth through modulation of microtubule dynamics. Neuron 56:604–620.

Mitchison T, Kirschner M (1984) Dynamic instability of microtubule growth. Nature 312:237–242.

Nakata K, Abrams B, Grill B, Goncharov A, Huang X, Chisholm AD, Jin Y (2005) Regulation of a DLK-1 and p38 MAP kinase pathway by the ubiquitin ligase RPM-1 is required for presynaptic development. Cell 120:407–420.

Pierre S, Maeurer C, Coste O, Becker W, Schmidtko A, Holland S, Wittpoth C, Geisslinger G, Scholich K (2008) Toponomic analysis of functional interactions of the ubiquitin ligase PAM (protein associated with Myc) during spinal nociceptive processing. Mol Cell Proteomics 7:2475–2485.

Purro SA, Ciani L, Hoyos-Flight M, Stamatakou E, Siomou E, Salinas PC (2008) Wnt regulates axon behavior through changes in microtubule growth directionality: a new role for adenomatous polyposis coli. J Neurosci 28:8644–8654.

Rajnicek AM, Foubister LE, McCaig CD (2006) Growth cone steering by a physiological electric field requires dynamic microtubules, microfilaments and Rac-mediated filopodial asymmetry. J Cell Sci 119:1736–1745.

Rothenberg ME, Rogers SL, Vale RD, Jan LY, Jan YN (2003) *Drosophila* pod-1 crosslinks both actin and microtubules and controls the targeting of axons. Neuron 39:779–791.

Sabry JH, O'Connor TP, Evans L, Toroian-Raymond A, Kirschner M, Bentley D (1991) Microtubule behavior during guidance of pioneer neuron growth cones in situ. J Cell Biol 115:381–395.

Salinas PC, Zou Y (2008) Wnt signaling in neural circuit assembly. Annu Rev Neurosci 31:339–358.

Samson F, Donoso JA, Heller-Bettinger I, Watson D, Himes RH (1979) Nocodazole action on tubulin assembly, axonal ultrastructure and fast axoplasmic transport. J Pharmacol Exp Ther 208:411–417.

Schaefer AM, Hadwiger GD, Nonet ML (2000) rpm-1, a conserved neuronal gene that regulates targeting and synaptogenesis in *C. elegans*. Neuron 26:345–356.

Schaefer AW, Kabir N, Forscher P (2002) Filopodia and actin arcs guide the assembly and transport of two populations of microtubules with unique dynamic parameters in neuronal growth cones. J Cell Biol 158:139–152.

Schaefer AW, Schoonderwoert VT, Ji L, Mederios N, Danuser G, Forscher P (2008) Coordination of actin filament and microtubule dynamics during neurite outgrowth. Dev Cell 15:146–162.

Suh LH, Oster SF, Soehrman SS, Grenningloh G, Sretavan DW (2004) L1/Laminin modulation of growth cone response to EphB triggers growth pauses and regulates the microtubule destabilizing protein SCG10. J Neurosci 24:1976–1986.

Tanaka EM, Kirschner MW (1991) Microtubule behavior in the growth cones of living neurons during axon elongation. J Cell Biol 115:345–363.

Tsui HT, Lankford KL, Ris H, Klein WL (1984) Novel organization of microtubules in cultured central nervous system neurons: formation of hairpin loops at ends of maturing neurites. J Neurosci 4:3002–3013.

Wan HI, DiAntonio A, Fetter RD, Bergstrom K, Strauss R, Goodman CS (2000) Highwire regulates synaptic growth in *Drosophila*. Neuron 26:313–329.

Williamson T, Gordon-Weeks PR, Schachner M, Taylor J (1996) Microtubule reorganization is obligatory for growth cone turning. Proc Natl Acad Sci U S A 93:15221–15226.

Yvon AM, Wadsworth P, Jordan MA (1999) Taxol suppresses dynamics of individual microtubules in living human tumor cells. Mol Biol Cell 10:947–959.

Zhen M, Huang X, Bamber B, Jin Y (2000) Regulation of presynaptic terminal organization by *C. elegans* RPM-1, a putative guanine nucleotide exchanger with a RING-H2 finger domain. Neuron 26:331–343.

Zhu S, Korzh V, Gong Z, Low BC (2008) RhoA prevents apoptosis during zebrafish embryogenesis through activation of Mek/Erk pathway. Oncogene 27:1580–1589.